Ionospheric code delay estimation in a single frequency case for Civil Aviation

Christophe Ouzeau, Frédéric Bastide, Christophe Macabiau, Benoit Roturier

HAL Id: hal-01021789
https://enac.hal.science/hal-01021789

Submitted on 31 Oct 2014

Ionospheric Code Delay Estimation in a Single Frequency Case for Civil Aviation

Christophe Ouzeau, *ENAC/TéSA/DTI*
Frédéric Bastide, *Sofréavia/DTI*
Christophe Macabiau, *ENAC*
Benoît Roturier, *DSNA-DTI*

BIOGRAPHIES

Christophe OUZEAU received a master in astronomy with gravitational systems dynamics speciality at the Observatory of Paris. In 2005, he began his Ph.D. thesis on degraded modes resulting from the multiconstellation use of GNSS, supported by DTI and supervised by ENAC.

Frédéric BASTIDE graduated in July 2001 as an electronics engineer from the Ecole Nationale de l'Aviation Civile (ENAC) in Toulouse, France. He received his PhD in 2004, his researches focus on combined GPS and GALILEO receivers.

Christophe MACABIAU graduated as an electronics engineer in 1992 from the ENAC in Toulouse, France. Since 1994, he has been working on the application of satellite navigation techniques to civil aviation. He received his PhD in 1997 and has been in charge of the signal processing lab of the ENAC since 2000.

Benoît ROTURIER graduated as a CNS systems engineer from Ecole Nationale de l'Aviation Civile (ENAC), Toulouse in 1985 and obtained a PhD in Electronics from Institut National Polytechnique de Toulouse in 1995. He was successively in charge of Instrument Landing Systems at DGAC/STNA (Direction Générale de l'Aviation Civile/Service Technique de la Navigation Aérienne), then of research activities on CNS systems at ENAC. He is since 2000 head of GNSS Navigation subdivision at DGAC/DTI (Direction de la Technique et de l'Innovation, formerly known as STNA) and is involved in the development of civil aviation applications based on GPS/ABAS, EGNOS and GALILEO. He is also currently involved in standardization activities on future multiconstellation GNSS receivers within Eurocae WG62 and is the chairman of the technical group of ICAO Navigation Systems Panel.

ABSTRACT

Ionosphere is a dispersive medium that can strongly affect GPS and GALILEO signals.

Ionospheric delay affecting the GPS and GALILEO pseudorange measurements is the larger source of ranging error, if left uncorrected. In addition, this perturbation is difficult to model and thus difficult to predict.

A multi-frequency receiver can identify and correct errors induced by the ionosphere, as in the nominal case, two frequencies are sufficient to determine precisely the ionospheric delay. However, if affected by radio frequency interference, a receiver can lose one or more frequencies leading to the use of only one frequency to estimate ionospheric code delay. Therefore, it is felt by the authors as an important task to investigate techniques aimed at sustaining multi-frequency performance when a multi-constellation receiver installed in an aircraft is suddenly affected by radiofrequency interference, during critical phases of flight.

The case of a loss of all but one frequency is studied in [Shau-Shiun Jan, 2003]. In this case, the usual code-carrier divergence technique is analyzed, consisting in computing the difference between the signal code and the carrier phase measurements. This difference is twice the ionospheric delay plus ambiguity plus errors, from which the ionospheric delay can be extracted. If a cycle slip occurs, the integer ambiguity appearing as a constant offset in the code-carrier difference causes this technique not to be valid. In the case of a single frequency receiver, a Kalman filter can be used to determine if a cycle slip occurs, introducing ambiguities of all satellites in view in the state vector as mentioned in [Lestarquit, 1995]. This Kalman filter can be initialized in the dual frequency mode, and left running when only one frequency is left.

The aim of this paper is first to propose a method for single frequency ionospheric delay estimation after the loss of multiple frequency tracking, and also to analyse the performance of this method with regards to the civil aviation requirements. The proposed technique includes the detection of cycle slips.

INTRODUCTION

In a future civil aviation nominal case, dual frequency GPS measurements allow to directly estimate ionospheric code delay from pseudorange measurements.

One can obtain ionospheric error via a linear combination of the pseudoranges at two different frequencies (defined by the index 1 and 2):

$$P = \frac{f_1^2}{f_1^2 - f_2^2} P_1 - \frac{f_2^2}{f_1^2 - f_2^2} P_2$$

$$\phi = \frac{f_1^2}{f_1^2 - f_2^2} \phi_1 - \frac{f_2^2}{f_1^2 - f_2^2} \phi_2$$

This « iono-free » combination allows suppressing ionosphere error term in pseudoranges or in phase expressions.

However, in case of radiofrequency interference (RFI) for instance, the loss of one frequency may be a problem if one want to keep the same performance as in the nominal dual frequency case and so we need to use alternate techniques to estimate the ionospheric error.

Carrier phase measurements are provided by carrier tracking loops. Measurements depend on the loop ability to give an approximate value close to the actual value of the carrier phase.

In a nominal case, this loop is able to quickly follow the time evolution of the incoming phase, and measurement errors are small. However, the tracking loop may lose the signal during a short period and then re-acquire it just after the break. The phase ambiguity will therefore vary in this case. This problem, called cycle slip, occurs when the C/N0 is low (antenna gain, obstacle,…) or when the receiver has too important and unpredictable movements. Such a phenomenon causes a phase jump (cycle slip) and can be modelled by a rupture, a sudden change from one measurement to the next one.

As we will see in the following part, a single frequency method can provide a good estimation of ionospheric error but it is not the case if cycle slips occur.

1. GLOBAL STRATEGY

In the dual frequency civil aviation case, smoothed iono-free range measurements are used. The ionospheric error is estimated and corrected thanks to the use of dual frequency.

In the case of loss of one frequency (degraded mode), an estimation of the ionospheric delay may be provided either by the Klobuchar model for GPS or the NeQuick one in case of Galileo. But, they only estimate part of the ionospheric error (Klobuchar ~50% and NeQuick ~80%). This implies use of large σ_{UERE} values, that do not allow supporting flight operations that require vertical protection levels computation (degraded mode).

But, in single frequency, can we keep the accuracy of the ionospheric delay estimation compatible with critical phases of flight (APV) just after the loss of dual frequency ?

We have analyzed the feasibility of precisely estimating the ionospheric delay in single frequency mode. It appears that Code Minus Carrier divergence technique is the most promising technique that may be used as mentioned in [Nats, 2003]. We describe this technique further in this paper. The characteristics of this technique are that it doesn't need an ionospheric model but carrier phase ambiguities have to be removed from the estimation to get ionospheric delay. If a cycle slip occurs, phase measurements are biased in consequence and estimations must be corrected so as to provide a good estimation of ionospheric code delay. In the following parts, we will see how to improve Code Minus Carrier divergence technique. The challenge here is to detect and correct cycle slips with regards to ICAO requirements.

Let's first describe the Code Minus Carrier divergence technique.

2. CODE MINUS CARRIER DIVERGENCE TECHNIQUE

After a loss of several frequencies leading to a single frequency degraded mode, resulting from a perturbation like interference, a receiver can use code and carrier phase pseudoranges made on only one carrier frequency. To estimate ionospheric delay, we can use the difference between code and carrier phase measurements. This is modelled as (x frequency):

$$P_x - \phi_x = 2I_x - N_x \lambda_x + w_x + v_x$$

where
- P is the code pseudorange measurement in meters
- ϕ is the phase measurement in meters
- I is the ionospheric delay in meters
- N is the integer ambiguity
- λ is the carrier wavelength in meters
- w is the code multipath and noise error
- v is the phase multipath and noise error

Indeed the difference between code delay and phase advance provides us two times the shift

caused by the ionosphere propagation of the electromagnetic waves.

The ionospheric delay can therefore be extracted from this difference assuming N is constant. This is the so-called code minus carrier divergence technique.

We make the assumption that v_x and w_x only depend on noise and multipath i.e. that clock errors at the receiver and satellite levels, tropospheric errors get cancelled in the difference computation.

The ionospheric delay can be extracted from that difference, provided the ambiguity is known and constant, i.e. no cycle slip occurs.

If a cycle slip occurs, the code carrier divergence method is not adapted to this situation as phase measurements are biased differently. It is therefore necessary to be able to determine exactly when this type of phenomenon occurs, whatever atmospheric conditions.

Cycle slips may have various causes, for instance multipath and ionospheric scintillation, or receiver dynamics as mentioned previously.
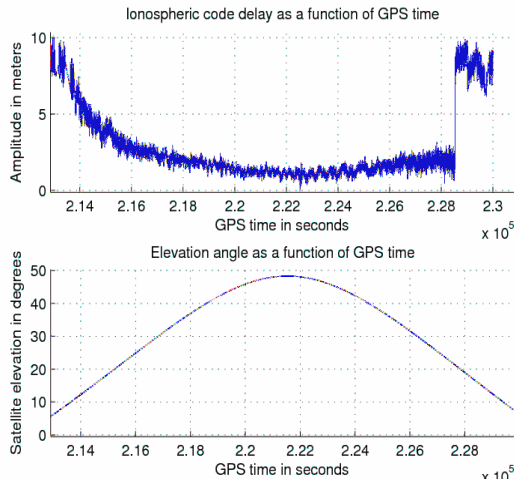

Figure 1: Amplitude of L1 ionospheric delay for a receiver located at ENAC, Toulouse, France, on 14/03/2006. A cycle slip occurs for a low elevation angle of about 20 degrees, which may correspond to a multipath.

Figure 1 shows the estimation of ionospheric code delay using single frequency CMC estimation on L1, we can note that a cycle slip occurs for a low elevation angle.

Those examples are known to generate cycle slips, but the amplitudes of the generated ruptures strongly vary from case to case. It would be possible to detect high amplitude cycle slips but it is really hard to detect small ones that don't allow estimating correctly ionosphere code delay with regards to civil aviation requirements in terms of integrity, for critical phases of flight.

We will now focus on cycle slip detection probability at the receiver level and cycle slip behaviour.

We use a Kalman filter in order to evaluate the ionosphere behavior and to follow the evolution of ambiguities of all satellites in view.

We define a state vector as in [Nisner, 1995] or [Lestarquit, 1995]:

$$X = \begin{bmatrix} I_0 & A & B & N_1 & ... & N_n \end{bmatrix}^T$$

where
- A and B are the linear gradients of ionospheric delay. A is constant within North-South axis and B is constant within East-West axis.
- I_0 is the ionospheric delay at the zenith of the receiver.

The obliquity factor, function of the elevation of each satellite in view; allows passing from slant value to vertical value (zenith). The obliquity factor is:

$$Ob = \left[1 - \left(\frac{R_e}{R_e + h} \cos(E) \right)^2 \right]^{-\frac{1}{2}}$$

where R_e is the Earth equatorial radius, h the altitude and E the elevation angle.

So from each CMC, we use the obliquity factor to compute the I_0 value so as to have a zenithal estimation for each satellite in view. Then, we compute the mean value of all obtained zenith ionospheric code delays.

The Kalman filter provides real time estimation of the ionospheric delay thanks to measurements from all satellites in view and of ambiguities for these satellites for the same frequency.

The relation between observation vector Y and state vector X at the instant t will be:

$$Y_t = H_t X_t + V_t$$

where
- Y_t is the observation vector, composed of the difference between code and carrier phase measurements for all satellites in view. Note that the obliquity factor is multiplied by two in the algorithm for the construction of the matrix H so as to obtain two times the ionospheric code delay: $Ob' = Ob * 2$ for each satellite.
- V_t is the observation noise

- H_t is the observation matrix which takes into account spatial and temporal correlations of the system at the instant t.

$$H = \begin{pmatrix} Ob_1' & Ob_1'\Delta\mu_1 & Ob_1'\Delta\lambda_1 & 1 & \dots & 0 \\ \vdots & \vdots & \vdots & \vdots & 1 & \vdots \\ Ob_n' & Ob_n'\Delta\mu_n & Ob_n'\Delta\lambda_n & 0 & \dots & 1 \end{pmatrix}$$

The first column of this matrix corresponds to the obliquity factor, the second and third ones correspond to the difference between two consecutive positions in latitude and longitude, i.e. $\Delta\lambda_i$ is the distance of the ionosphere piercing point from the receiver in the North-South direction and $\Delta\mu_i$ is the distance of the ionosphere piercing point from the receiver in the East-West direction, for the ith satellite. The index corresponds to the satellite index, n is the total number of satellites in view.

The state transition equation is

$$X_{t+1} = F_t X_t + W_t$$

For a first approach, F is taken equal to the identity (we suppose that in nominal case, no variations occur in state vector).

W is a noise process, it is here to model random fluctuations in linear prediction model imperfections.

The covariance matrix of W is Q:

$$Q = \begin{pmatrix} \left(\frac{\Delta t}{720}\right)^2 & 0 & 0 & 0 & \cdots & 0 \\ 0 & \left(\frac{\Delta t}{1200}\right)^2 & 0 & \vdots & \ddots & \vdots \\ 0 & 0 & \left(\frac{\Delta t}{1200}\right)^2 & 0 & \cdots & 0 \\ 0 & \cdots & 0 & 1 & \cdots & 0 \\ \vdots & \ddots & \vdots & \vdots & \ddots & \vdots \\ 0 & \cdots & 0 & 0 & \cdots & 1 \end{pmatrix}$$

The covariance matrix of the measurement noise V is:

$$R = 3.5^2 * \begin{pmatrix} \left(\frac{Ob_1}{\Delta t}\right)^2 & \cdots & 0 \\ \vdots & \ddots & \vdots \\ 0 & \cdots & \left(\frac{Ob_n}{\Delta t}\right)^2 \end{pmatrix}$$

where Δt is the measurement interval, 3.5 is a multiplicative empirical term used in [Lestarquit, 1995].

When the receiver loses track of one satellite signal, its corresponding state in the state vector of the Kalman filter is suppressed, its ambiguity is not kept in memory. When a new satellite signal appears, the state vector is redefined taking into account the corresponding ambiguity, that is to say, the ambiguity is added in the state vector and the Kalman filter is reinitialized, the initial state and covariance are redefined taking into account the new number of satellites, the previously defined matrix .

3. CYCLE SLIPS OCCURRENCE RATE

We focus on the occurrence of cycle slips in the phase data. We define a flow events which are cycle slips occurring successively and separated by random time intervals. This process has Poisson characteristics.

So the probability of occurrence during Δt will be:

$P_{OCC} = \exp(-\overline{T}\Delta t)$ where $\overline{T}$ is the cycle slip rate.

The probability of having K cycle slips during Δt:

$$P_{OCC}(K, \Delta t) = (\overline{T}\Delta t)^K \frac{\exp(-\overline{T}\Delta t)}{K!}$$

$\overline{T}$ is the mean time between two cycle slips.
σ_ϕ is the phase loop noise, its value depends on the type of loop employed:
- For a Costas loop,

$$\sigma_\phi = \sqrt{\frac{W_L}{\frac{C}{N_0}}\left(1 + \frac{1}{2\frac{C}{N_0}T_D}\right)}$$

- For a classical PLL,

$$\sigma_\phi = \sqrt{\frac{W_L}{\frac{C}{N_0}}}$$

where
- C/N_0 is the carrier to noise density ratio
- T_D is the coherent integration time
- W_L is the loop bandwidth

We can note that this last value of σ_ϕ does not depend on integration time for a classical PLL, but in reality, the integration will play a role for the normalization of the PLL discriminator.

The cycle slip rate (or cycle slip mean time) is computed using the following formula:

$$\overline{T} = \frac{\pi}{2W_L\gamma}\tanh\left(\frac{2\pi\gamma}{\sigma_\phi^2}\right)\times\left[\begin{array}{c}I_0^2\left(\dfrac{1}{\sigma_\phi^2}\right)+\\[2ex]2\displaystyle\sum_{n=1}^{\infty}(-1)^n\dfrac{I_n^2\left(\dfrac{1}{\sigma_\phi^2}\right)}{1+\left(\dfrac{n\sigma_\phi^2}{\gamma}\right)^2}\end{array}\right]$$

where I_n are Bessel functions of order n.

See [Holmes, 1990] for a complete demonstration. γ represents the tracking error of the phase linked to the receiver dynamic (rad), that is to say when the receiver moves, for instance, in an aircraft.

The rate of occurrence is then defined as the inverse of the cycle slip mean time $\overline{T}$.

For GNSS signals, we first compared the probabilities of occurrence of cycle slips using a Costas loop. This is shown in tables 1 and 2.

Signal type	Td	Probability of occurence within 150s
GPS L1 C/A	20 ms	5.3 e-004
GPS L5	20 ms	8e-004
GALILEO L1	100 ms	5.3e-004
GALILEO E5b	100 ms	7.7e-004

Signal type	Td	Probability of occurence within 150s
GPS L1 C/A	10 ms	5.3e-004
GPS L5	10 ms	8e-004
GALILEO L1	10 ms	5.3e-004
GALILEO E5b	10 ms	7.6e-004

Tables 1 and 2: Probability of cycle slip occurrence for a Costas PLL, with 10 Hz bandwidth, jerk max of 0.74 g/s, as a function of coherent integration time Td.

In tables 1 and 2, probability of occurrence of cycle slip is shown for different signals and integration times, for a Costas loop. During the same observation period (150 seconds), the probability of having a large number of cycle slips decreases exponentially.

Table 1 provides the probabilities of occurrence using coherent integration time corresponding to one code period. The second table shows the same probabilities but with a minimum integration time of 10 ms. We can see that there is little difference when the integration time is decreased down to 10 ms.

Note that future Galileo L1, E5a and E5b will include both dataless and pilot channels. In this case, no navigation data will modulate the pilot signal, so, the tracking loop will be sensitive to 180 degrees phase jumps after pilot code removal, consequently, a traditional PLL can be employed. So, the value of σ_ϕ won't vary as a function of integration time in the probability of occurrence computation.

Dynamics of the onboard receiver differs from case to case and depends on phases of flight. In order to be as exhaustive as possible, we will sweep all cases, choosing all possible dynamics parameters. Those values are provided by [MOPS, 2006] white paper and are recalled below:

Ground speed	800 Kt
Horizontal acceleration	0.58 g
Vertical acceleration	0.5 g
Total jerk	0.25 g/s

Table 4: normal aircraft dynamics, [MOPS, 2006].

Ground speed	800 Kt
Horizontal acceleration	2.00 g
Vertical acceleration	1.5 g
Total jerk	0.74 g/s

Table 5: abnormal manoeuvres, [MOPS, 2006].

Where g = 9.81m/s² and Kt are Knots.

The probability of occurrence of cycle slips within 150 seconds (critical phase of flight duration) is computed using Holmes formula for maximum jerk from normal to abnormal manoeuvres.
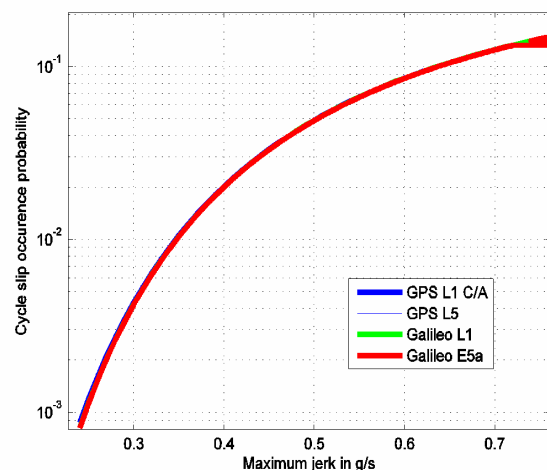

Figure 4: Probability of occurrence of cycle slip during 150 seconds.

As a conclusion, the probability of a cycle slip to occur is low but not negligible for civil aviation purposes. It has a behaviour that follows Poisson

law. The probability of having K cycles slips within a given period is decreasing exponentially with K.

Furthermore, the probability of a multipath to occur is dependent on the phase of flight for an aircraft and the environment geometry and structure. In addition, cycle slips occurrence depends on amplitude of multipaths but also other phenomena such as ionospheric scintillation, which amplitudes strongly vary. The probability of occurrence strongly depends on dynamics as shown in figure 4.

4. CIVIL AVIATION REQUIREMENTS

We define the integrity risk as the product of the probability of occurrence of cycle slips by the probability of missed detection of those jumps in carrier phase measurements. So, regarding civil aviation requirements for integrity, we must determine first the probability of occurrence of cycle slips, then, the probability of missed detection and finally, the smallest detectable cycle slip with the required computed probability of missed detection. Similarly, false alarm rate is determined from ICAO continuity requirements.

In civil aviation, the integrity monitoring algorithm generally involves two functions which are anomaly detection and exclusion. Those functions allow GNSS navigation to continue without service interruption.

This algorithm depends upon the desired missed detection and false alarm probabilities. Computation of protection levels are assured by the computation of those probabilities.

We will focus on the transition from NPA to APV phases of flight.

Below is presented ICAO requirements for those phases of flight.

For APV I and APV II approaches, the value of the probability of missed detection is deduced from the integrity risk and the probability of occurrence of cycle slips. The integrity risk equals $2*10^{-7}$ /approach. This value is the same for GPS or GALILEO standalone and GPS/GALILEO combined constellation see [MOPS, 2006].

Allowed false alarm probability is determined from continuity ICAO requirements. In [RTCA, 2006], the false alert probabilities are set to $3.33 \cdot 10^{-7}$/sample and $1.6 \cdot 10^{-5}$/sample for NPA and APV phases of flight, respectively. These values are higher than those assumed in simulations; they would lead to less continuity performance but improved availability.

Here we recall the performances required by ICAO for APV phases of flight:

	HAL	VAL	TTA
APV I	40 m	50 m	10 s
APV II	40 m	20 m	6 s

Table 6: Integrity requirements, [MOPS, 2006].

HAL stands for Horizontal Alert Limit, VAL for Vertical Alert Limit and TTA for Time To Alert.

The smallest detectable cycle slip we will be able to detect will give us an idea of the amplitude of the undetectable error in positioning, but this error will depend upon the geometry defined by the positions of the satellites and the receiver.

5. SMALLEST DETECTABLE CYCLE SLIP

To determine the smallest detectable bias with the required Pmd, we launch simulations to determine the performance of some cycle slip detection algorithms.

Different magnitudes of cycle slips must be simulated, and we have to compute non-detection probability and to determine whether the obtained values are acceptable as a function of magnitude of cycle slips.

We generate code, phase and Doppler measurements. Phase measurements were generated taking into account dynamics:

$$\Phi(t) = \rho_0 + v \times t + a \times 9.81 \times t^2 + j \times 9.81 \times t^3$$
$$+ b + multipath + atmosphere + noise$$
$$P(t) = \rho_0 + v \times t + a \times 9.81 \times t^2 + j \times 9.81 \times t^3$$
$$+ b + multipath + atmosphere + noise$$

Where:

- ϕ is the phase measurement in meters
- P is the code pseudorange measurement in meters
- ρ_0 is a typical constant range (ex: 20000 km)
- v is the range rate, taken here to be 800 + 70 m/s (worst case range rate due to satellite and aircraft movement during an approach).
- a is the acceleration. It is taken according to table 4 for normal maneuvers or table 5 for abnormal maneuvers.
- j is the jerk. It is taken according to table 4 for normal maneuvers or table 5 for abnormal maneuvers.
- b is the satellite clock bias generated as described in [Winkel, 2000].

The Doppler measurements were generated as a first order derivative of the previously defined phase but the additive noise is provided by Gaussian random values multiplied by a FLL sigma value defined in [Kaplan, 1996] instead of a PLL sigma value:

$$\sigma_{FLL} = \frac{1}{2\pi T_D} \sqrt{\frac{8W_L}{\frac{C}{N_0}}\left(1 + \frac{1}{T_D \frac{C}{N_0}}\right)} \; (Hz)$$

The multipath is generated by drawing Gaussian random values with a sigma corresponding to the worst case sigma at 5° elevation using [SARPs, 2006] formula:

$$\sigma_{multipath} = 0.13 + 0.53 * e^{-\frac{E}{10}}$$

The atmosphere is generated by drawing Gaussian random values with sigmas (see [Shau-Shiun Jan, 2003] corresponding to troposphere:

$$\sigma_{troposphere} = \frac{0.12 * 0.001}{\sqrt{0.002001 + \sin(E)^2}} \; with$$

an elevation angle E of 5 degrees, and ionosphere:

$$\sigma_{ionosphere\_phase} = 0.02m$$

$$\sigma_{ionosphere\_code} = 0.83m$$

The noise is generated as random gaussian values with a sigma corresponding the standard deviation of the tracking error due to noise.

We propose to define the following performances criteria of the algorithms of detection (and estimation).

First, the cycle slip detection and correction ability will be defined by the smallest cycle slip detectable with a required probability of missed detection, the false alarm rate. Other performance criteria are the robustness to carrier-to-noise ratio, multipath and receiver dynamics, the capability to dissociate several near slips and to correct those slips. Generally, those parameters have an influence on the performance of the technique of detection.

Secondly, the accuracy of ionospheric delay has to be considered regards to carrier-to-noise ratio and multipath.

Finally, the time computation cost of the algorithms must be taken into account, for instance with regards to Time To Alert for critical phases of flight, but this point concerns the future GNSS receivers architecture.

We won't verify all those criteria in this study but only the most critical ones, like resistance to

dynamics and smallest detectable cycle slip. If the technique is found interesting, further investigations may take into account all those criteria.

6. DETECTION USING PREDICTED PHASE MEASUREMENTS

The first algorithm is based on a prediction of future phase measurements with Doppler measurements:

$$\hat{\phi}(t) = \phi(t - \Delta t) + f_d(t - \Delta t) \times \Delta t$$

where f_d is the Doppler frequency and Δt is the time delay between the previous and the current measurement.

Then the difference between phase measurements and predicted phase measurements is compared to a threshold which has to be fixed:

$$\left|\hat{\phi}(t) - \phi(t)\right| > Threshold$$

The choice of a threshold is function of false alarm probability with regards to APV phase of flight requirement and depends on the receiver dynamics.

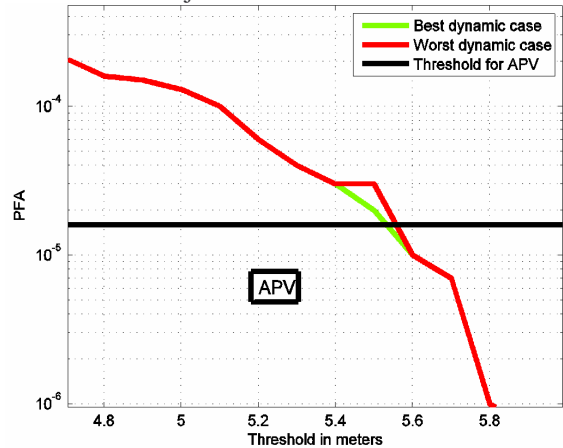Figure 5 shows the results obtained for varying acceleration and jerk.

Figure 5: Probability of False Alarm as a function of amplitude of cycle slips.

For APV, maximum integrity risk equals 2.10^{-7} per approach for GPS or GALILEO standalone or combined GPS/GALILEO. As the integrity risk is not only allocated to cycle slips, we choose to overbound the required probability of missed detection with a value of 10^{-5} for normal maneuvers and 10^{-6} for abnormal case. Now we have to determine the smallest detectable cycle slip with this required P_{MD}, using detection algorithms. Those values are represented respectively in green and red in the following figure.
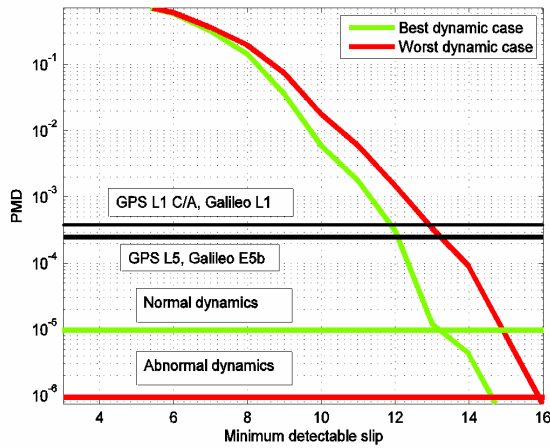
Figure 6: probability of Missed Detection with regards to integrity requirements for APV.

As we can see from figure 6, the smallest detectable cycle slips have an amplitude of 13 meters for normal dynamics and 16 meters for abnormal maneuvers, choosing a maximum jerk for those two cases.

As we mentioned above, the phase measurements were generated considering maximum acceleration and jerk values for all types of maneuvers. The inclusion of dynamics parameters (acceleration in t^2, jerk in t^3...) in pseudoranges implies that the detection is much more difficult than for a static receiver (which minimum detectable cycle slip amplitude is under a meter as mentioned in [Hegarty, 1993]), this results here in a minimum detectable cycle slip of a few meters.

These smallest detectable cycle slips imply a bias on position error depending on geometry. Availability of protection against cycle slip compatible with APV I and APV II depends on geometry and must be computed at every second. The ICAO requirements for those phases of flight are recalled in the section 4 of this paper.

7. KALMAN FILTER + GLR

A cycle slip induces a rupture in the innovation vector level, that is to say a sudden variation from one instant to another. Such a rupture may be detected only a posteriori.

Let's define X_t and I_t respectively as the state and innovation vectors at the instant t without any rupture.

When a state parameter changes (for instance an ambiguity value), variations will be described by additive parameters in state and innovation vectors:

$$\begin{cases} X_t(r) = X_t + State\_change \\ \\ I_t(r) = I_t + Innovation\_change \end{cases}$$

where r is the rupture instant and t the current instant.

In order to determine events that could affect state in the Kalman filter, a technique used is the generalized likelihood ratio proposed by Willsky in [Willsky, 1976]. This technique has been developed for linear systems, but we can use it when the state is estimated by a Kalman filter or an extended Kalman filter.

In order to apply the generalized likelihood ratio technique, let's formulate the problem.

A state break may be represented by an abnormal fluctuation of the innovation I of the Kalman filter. This jump in the mean is a response to a state impulsion of the deterministic system defined by the matrix couple: (H, F) which are defined by the Kalman system.

Let's define a rupture as an additional term in the state vector:

$$\hat{X}_{t|t}(r) = \hat{X}_{t|t} + \beta_X(t,r)$$
$$\beta_X(t,r) = \mu_X(t,r)\nu_X$$

where k is the considered instant and r the instant of a potential rupture which occurred before k, $\hat{X}_{t|t}(r)$ is the estimation of the state vector with a rupture which occurred at r, $\hat{X}_{t|t}$ is this estimation without rupture and $\beta_X(t,r)$ is the additive perturbation at the instant t which occurred at r on the state vector X. $\mu_X(t,r)$ will be defined further in this document.

ν_X is the magnitude of a potential jump and μ defines the difference between state vector value in nominal case (without jump) and in case of a jump which occurred and a previous instant r.

We also write the effect of a potential rupture on the innovation vector:

$$I_t(r) = I_t + \rho_X(t,r)$$
$$\rho_X(t,r) = \varphi_X^T(t,r)\nu_X$$

where φ is defined in the same manner than μ, we will further describe those terms.

The GLR algorithm (Generalized Likelihood Ratio) allows estimating additive changes on a state.

The main interest in such an algorithm is that we can determine both the time when a rupture occurs and its magnitude.

This algorithm has two main operations:

- Detection: it is based on a multiple hypothesis test examining all the possible mean jumps on each instant k since the initial instant t0 (t0 = 1 for instance). The hypothesis H_0 corresponds to the case when no rupture occurs within [t0, k]. The other complementary hypothesis is when a rupture occurs. The statistic test is defined as the likelihood ratio. The best candidate for a selected rupture is the index of the maximum value of this ratio. However, as the magnitude of a rupture is unknown, it's replaced by its estimation obtained with the maximum of likelihood computed under the H_1 hypothesis. A decision is taken comparing the likelihood ratio for the chosen magnitude and time index with a defined threshold.
- Compensation: if a rupture is detected, Kalman filter state vector is corrected to take into account the induced error.

If we note I_t the innovation obtained with a Kalman filter at the instant t and r the instant of a potential structure, the estimations of magnitude and time index of this rupture are provided by:

$$\hat{v}(r) \;=\; \arg \; \max_{v} \; \log \; \frac{p(I_1^t \mid r, v)}{p(I_1^t \mid H_0)}$$

and

$$\hat{r} \;=\; \arg \; \max_{r} \; \log \; \frac{p(I_1^t \mid r, \hat{v}(r))}{p(I_1^t \mid H_0)}$$

where I_1^t represents the innovation sequence within [1, t].

Let's define φ and μ the regressive parameters as:

$$\varphi_X^T(t+1, r)v_X \;=\; I_{t+1}(r) - I_{t+1}$$
$$= H_{t+1}(X_{t+1}(r) - X_{t+1}) - H_{t+1}(\hat{X}_{t|t}(r) - \hat{X}_{t|t})$$
$$= H_{t+1}(\prod_{i=r}^{t} F_i - F_t \mu_X(t,r))v_X$$

And :

$$\mu_X^T(t+1, r)v_X \;=\; \hat{X}_{t+1|t+1}(r) - \hat{X}_{t+1|t+1}$$
$$= F_t(\hat{X}_{t+1|t+1}(r) - \hat{X}_{t+1|t+1}) - K_{t+1}(I_{t+1}(r) - I_{t+1})$$
$$= F_t \beta_X(t,r) + K_{t+1}\rho_X(t+1, r)$$
$$= (F_t \mu_X(t,r) + K_{t+1}\varphi_X^T(t+1, r)v_X$$

Innovation has a zero-centered normal distribution when no rupture occurs. This law is translated when a rupture occurs; it's a $\rho(t,r)$- centered normal distribution.

For a change test, in an innovation I_t, $I_t(r) = I_t + \rho(t,r)$, the log likelihood ratio is defined by:

$$l_t(r, \hat{v}(r)) \;=\; 2 \log \; \frac{p(I_1^t \mid r, \hat{\rho}_1^t(r))}{p(I_1^t \mid H_0)}$$
$$= \sum_{i=r+1}^{t} I_i^T \Sigma_i^{-1} I_i - (I_i - \hat{\rho}_i(r))^T \Sigma_i^{-1}(I_i - \hat{\rho}_i(r))$$

where Σ_i is the covariance of I_i.

All the factors are computed in a recursive manner within a M-sized window.

The initialization of the algorithm is provided by:

$$\zeta(t,t) = K_t H_t$$
$$\rho(t,t) = H_t$$

If we define:

$$d_X(t, r) = \sum_{i=1}^{t} \varphi_X(i, r)\Sigma_i^{-1} I_i$$

and

$$C_X(t, r) = \sum_{i=1}^{t} \varphi_X(i, r)\Sigma_i^{-1}\varphi_X^T(i, r),$$

We obtain another formulation of the previously defined likelihood ratio:

$$l_t(r, \hat{v}(r)) = d_X^T(t,r)C_X^{-1}(t,r)d_X(t,r),$$

and :

$$\hat{r} \;=\; \arg \; \max_{t-M+1 \le r \le t} \; l_t(r, \hat{v}(r))$$

An error is then detected when $l_t(\hat{r}, \hat{v}(\hat{r}))$ is greater than a predefined threshold.

The comparison between the likelihood ratio and a threshold λ will allow to choice one of the two hypotheses.

The parameters for the algorithm implementation are the decision threshold (to compare with the likelihood ratio) and the decision window size and its translation step.

The choice of a good threshold could allow obtaining good performances so as to ensure detection process is both robust and accurate.

The decision threshold will depend on the cycle slip amplitude to signal ratio. This threshold has to be chosen in order to minimize false alarm probability and, at the same time, to minimize missed detection probability.

The window size determination depends upon the magnitude of a cycle slip compared with the mean variations of the signal. The more the magnitude rupture is large, the smaller the windows can be chosen as in this case, it is easy to identify a rupture. Furthermore, the detection window size must be as small as possible. Indeed, in case of cycle slip, ionospheric error estimation is biased and it results an error in position estimation so alert limits may be reached. In this case, and particularly during critical phases of flight, compared to time to alert (10 seconds for APV I for instance) the window size have to be as low as possible. This is all the more important since the fact time computation and reparation must be taken into account. This last time computation is one of the performance criteria mentioned above. This point must be discussed while verifying civil aviation protection levels and integrity requirements. Note that the more detection are made, the higher will be the time cost of the algorithm because of actualisation of Kalman filter state vector.

The previous algorithm using Doppler measurements is snapshot whereas this one is sequential so performance analysis needs to take into account the size of sliding window regards to Time To Alert which corresponds to 10 seconds for APV I and 6 seconds for APV II.

The detection capability is similar to the previous technique, but this method needs to be refined.

The problem is that the cycle slip estimation error increases with the magnitude of the cycle slip as shown in the following figure.
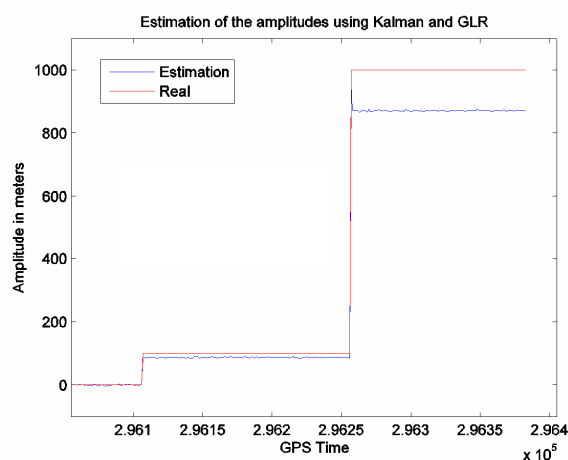

Figure 7: Estimated amplitude (in meters) of generated cycle slips in blue compared to real amplitudes generated in red using GLR.

8. CONCLUSION

We have analyzed the performance of ionospheric delay estimation in single frequency mode for civil aviation application.

The method used is the Code Minus Carrier divergence, and we are interested in accuracy of the method.

Cycle slip detection capability using Doppler measurements is not always compatible with APV I, APV II integrity requirements (smallest detectable cycle slip is 13 meters for normal dynamics and 16 meters for abnormal manoeuvres). Cycle slip detection capability with proposed Kalman Filter and GLR is similar to detection capability with Doppler measurements.

Future works include modifications in the proposed Kalman Filter in order to try and improve cycle slip detection capability or resistance to cycle slips (hybridization with Galileo NeQuick model, inclusion of dynamics).

ACKNOWLEDGMENTS

REFERENCES

[Hegarty, 1993] Hegarty Christopher J., "An Assessment of Alternative Methods of Mitigating Ionospheric Errors for WADGPS Users", MITRE Technical Report MTR93W111, The MITRE Corporation, McLean, Virginia, 1993.

[Holmes, 1990] Coherent Spread Spectrum Systems, Robert E.Krieger Publishing Company, Malabar, Florida, Holmes, 1990.

[Kalman, 1993] Kalman Filtering, Theory and Practice, Mohinder S.Grewal, Angus P. Andrews, Prentice Hall Information and System Sciences Series, Thomas Kailath, Series Editor.

[Kaplan, 1996] Understanding GPS, Principles And Applications, Elliott D.Kaplan, Artech House, Boston, London, 1996.

[Lestarquit, 1995] Determination of the Ionosphere Error Using Only L1 Frequency GPS Receiver, Laurent Lestarquit, Norbert Suard, Jean-Luc Issler, CNES, 1995.

[MOPS, 2006] Interim Minimum Operational Performance Specification For Aiborne Galileo Satellite Receiving Equipment, White Paper, EUROCAE, May 2006.

[NATS, 2003] Sustainable Mobility and Intermodality Promoting Competitive and Sustainable Growth, Maintaining Dual Frequency Navigation Performance in the Presence of Interference, 2003.

[Nisner, 1995] GPS Ionosphere Determination Using L1 Only, Paul Nisner, UK National Air Traffic Services, Mike Trethewey, Signal Computing Ltd, ION 1995.

[RTCA, 2006] Radio Technical Commission for Aeronautics, do229c, 2006.

[SARPs, 2006] Standards and Recommended Practices, ICAO, 2006.

[Shau-Shiun Jan, 2003] Aircraft Landing Using a Modernized Global Positioning System And The Wide Area Augmentation System, Shau-Shiun Jan, May 2003.

[Willsky, 1976] A.S. Willsky and H. L. Jones (1976). A generalized likelihood ratio approach to the detection and estimation of jumps in linear systems. IEEE Trans. Aut. Control, 21, pp. 108-112.

[Winkel, 2000] PhD Thesis dissertation, 2000.